A national laboratory of the U.S. Department of Energy
Office of Energy Efficiency & Renewable Energy

National Renewable Energy Laboratory

Innovation for Our Energy Future

Effects of Biodiesel Operation on Light-Duty Tier 2 Engine and Emission Control Systems

Preprint

M. Tatur, H. Nanjundaswamy, and D. Tomazic
FEV Inc.

M. Thornton
National Renewable Energy Laboratory

Presented at SAE 2008 World Congress
Detroit, Michigan
April 14–17, 2008

Conference Paper
NREL/CP-540-42928
August 2008

NREL is operated by Midwest Research Institute • Battelle Contract No. DE-AC36-99-GO10337

Effects of Biodiesel Operation on Light-Duty Tier 2 Engine and Emission Control Systems

Marek Tatur, Harsha Nanjundaswamy, Dean Tomazic
FEV Inc.

Matthew Thornton
National Renewable Energy Laboratory

ABSTRACT

Interest in diesel-powered passenger cars is rising in the United States, along with the desire to reduce the nation's dependence on imported petroleum. As a result, operating diesel vehicles on fuels blended with biodiesel is also gaining attention. One of several factors to consider when operating a vehicle on biodiesel blends is understanding the performance and impact of the fuel on the emission control system.

This paper documents the impact of biodiesel blends on engine-out emissions as well as overall system performance in terms of emission control system calibration and overall system efficiency.

The testing platform is a light-duty, high-speed, direct-injection diesel engine with a Euro 4 base calibration in a 1700-kg sedan vehicle. It employs a second-generation common-rail injection system with a peak pressure of 1600 bar, as well as cooled high-pressure exhaust gas recirculation. The study includes three different fuels: U.S. ultra-low-sulfur diesel (ULSD) base fuel, B5, and B20 prepared from soy-derived biodiesel. The study also includes two different emission control systems (ECS): oxides of nitrogen (NO_x) adsorber catalyst (NAC) with a diesel particle filter (DPF), and selective catalytic reduction with a DPF.

This paper focuses primarily on NAC calibration, regeneration, and desulfurization; DPF regeneration and preliminary emissions, focusing on NO_x; and fuel economy results. The NAC ECS aged to end-of-life conditions showed efficiencies in the mid-80% range, thus allowing operation within Tier 2 Bin 5 emission standards for both intermediate and useful life conditions.

Results of the vehicle chassis tests showed some NO_x benefits when operating on B20 fuel blends with the NAC ECS. This is a result of calibration work being performed using the 20% biodiesel fuel blend. The higher exhaust temperatures resulting from the use of ULSD resulted in lower ECS effectiveness with the NAC. The average tailpipe results when operating the vehicle on B20 were in the range of 0.03 g/mi, while the emissions with ULSD averaged below 0.05 g/mi with larger cycle-to-cycle variability.

INTRODUCTION

Because of advances in diesel engine technology, light-duty diesel-powered vehicles are becoming more popular in the United States. In addition to the increased interest in light-duty diesel vehicles, the anticipation and eventual phasing in of stringent Tier 2 emission standards for this vehicle class has led to a need for emission control systems (ECS) on these vehicles. Concurrently, increasing fuel prices have rejuvenated interest in biofuels, such as biodiesel, as a means to reduce or replace the demand for petroleum-derived fuels.

Selective catalytic reduction (SCR) with urea and oxides of nitrogen (NO_x) adsorber catalyst (NAC) are the leading technologies for meeting the Tier 2 NO_x emission standards for light-duty diesel vehicles. Extensive research conducted over the past decade has focused on the performance and durability of these technologies when used in vehicles operating on conventional fuels [1-8]. However, little research has been performed to gain an understanding of the impact of biofuels—or, more specifically, biodiesel—on ECS.

Biodiesel is a renewable fuel derived from vegetable oil, animal fat, or waste cooking oil; it consists of the methyl esters of fatty acids. It is typically used as a diesel blending component at levels up to 20 percent by volume. A resource assessment indicates that biodiesel has the potential to displace 5% or more of petroleum diesel over the next decade [9]. A life-cycle analysis indicates that the use of B20 fuel reduces life-cycle petroleum consumption by 19% [11]. However, little is known about the potential impacts of these fuel blends on the life and performance of ECS.

This paper discusses the emissions performance of the NAC system, combined with a diesel oxidation catalyst (DOC) and a diesel particle filter (DPF), while operating

on ultra-low-sulfur diesel (ULSD) and a blend of ULSD and 20% biodiesel (B20). A consideration of SCR and NAC chemistry suggests several areas in which biodiesel blends may perform differently than pure petroleum-derived fuels do. This paper includes an initial look at these potential areas, as well as a discussion of test-bed hardware, ECS specifications, controls, and initial emission results.

Before ECS development began, engine-out emissions were recalibrated to result in required NO_x and hydrocarbon (HC) conversion efficiencies of approximately 80% from the emission control system. The achieved target level was in the range of 0.35 g/mi NO_x emissions for Federal Test Procedure (FTP) 75.

Based on the experience gained during the Advanced Petroleum-Based Fuels-Diesel Emission Controls (APBF-DEC) light-duty vehicle development efforts [1, 2, 4, 7, 8], the development team decided to begin activities with implementation and calibration of the NAC system.

The hardware configuration was defined as a close-coupled DOC and NAC combination allowing the fastest possible catalyst light-off after a cold start. The SCR system was designed around the vehicle body constraints with a close-coupled DOC and an under-floor SCR-DPF, allowing sufficient mixing length after the point of injection for urea.

TESTING HARDWARE AND SOFTWARE

The testing was conducted primarily in the engine test cell running steady-state as well as transient test cycles simulation which includes all certification cycles such as the FTP75, the Highway Fuel Economy Test (HFET), and the US06 Supplemental Federal Test Procedure, a more aggressive driving cycle. This approach allowed an investigation of engine and emission control system behavior in great detail under controlled conditions. The results of all development activities were confirmed on a vehicle chassis dynamometer.

The U.S. Environmental Protection Agency (EPA) National Vehicle and Fuel Economy Laboratory (NVFEL) in Ann Arbor, Michigan, was used to determine the vehicle emissions performance over the certification cycles after the completion and integration of all development activities.

ENGINE HARDWARE - The engine used for this project is an in-line 4-cylinder, turbocharged, common-rail system direct-injected engine, producing 106 kW at 4000 rpm and peak torque of 360 Nm at 2000 rpm. The base engine hardware was a Euro 4 level configuration and was not modified during the development efforts. It consisted of a high-pressure exhaust gas recirculation (EGR) loop with the EGR cooler partially integrated in the cylinder head, as well as a variable-nozzle turbine (VNT) turbocharger.

All actuators were electronically controlled and used electric actuators for adjustments. Table 1 includes more detailed parameters.

Table 1: Engine specifications

Engine power	106 kW @ 4000 rpm
Peak torque	360 Nm @ 2000 rpm
Max. engine speed	4700 rpm
Max. BMEP	22 bar
Number & arrangement of cylinders	4-cylinder inline
Firing order	1 - 3 - 4 - 2
Valve train	4-valve DOHC
Displacement	2.15 L
Bore-to-stroke ratio	1.0034
Compression ratio	18
Fuel injection system	Second-generation common-rail DI

Figure 1 illustrates the engine's engine-out specific NO_x emissions over the entire engine map. The engine operates in conventional diesel mode without the use of low-temperature combustion techniques in certain engine operating regimes.

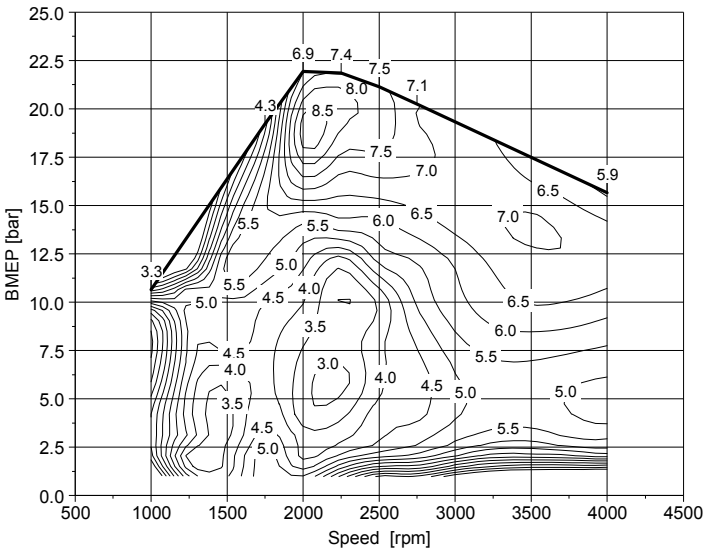

Figure 1: Engine-out NO_x [g/kWh]

VEHICLE SPECIFICATIONS - The vehicle used in this project is a mid-size four-door sedan with the base specifications listed in Table 2. No vehicle modifications, such as removal of components with the intent to decrease vehicle weight, were performed. The only modification was the installation of the rapid prototyping equipment required to control the ECS and the data acquisition system.

Table 2: Vehicle specifications

Criteria	*Unit*	*Value*
Vehicle mass	kg	1700
Air drag coefficient	-	0.29
Frontal surface area	m^2	2.20
Transmission gear ratio	1st	4.99
	2nd	2.82
	3rd	1.78
	4th	1.25
	5th	1.00
	6th	0.82
	Axle	2.65
Tires / Wheels	rear	205/55 R 16 91 H
	front	205/55 R 16 91 H

EMISSION CONTROL HARDWARE - As indicated, two different ECS were subject to evaluation as part of this project. The first system developed was a NAC system. An SCR system is also being developed, and results will be described in a later publication. In both cases, a close-coupled DOC and an under-floor DPF are included. Catalyst sizes were chosen that allowed manageable packaging on the project vehicle. All catalyst components were connected through dual-wall (air gap insulated) piping. The vehicle's original muffler remained in place.

The NAC system was composed of a close-coupled DOC/NAC combination (assembled in one can). This configuration enabled early catalyst light-off after cold start and thus fast and efficient control of gaseous emissions. The under-floor catalyzed DPF was also utilized to control any breakthrough hydrocarbons.

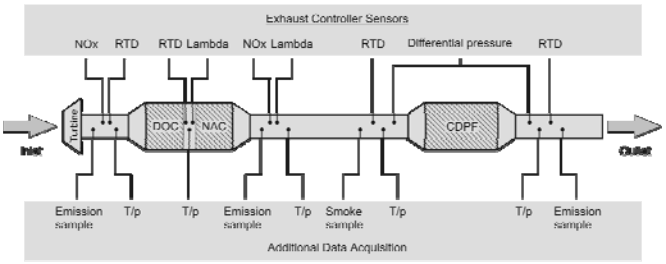

Figure 2: NO_x adsorber catalyst/DPF emission control system

Figure 2 shows the ECS layout and sensor suite used for controls at the top of the schematic and the additional sensor locations at the bottom. In order to provide the highest level of control accuracy and quality, a two-NO_x sensor setup was chosen. The removal of the upstream NO_x sensor and its replacement with an engine-out model is possible and was considered; this, however, results in some incremental decrease in system effectiveness, especially under highly transient conditions. Therefore, it was not utilized.

EMISSION CONTROL SOFTWARE - The design of the ECS software was intended to be as modular as possible. Each control module can be easily removed or substituted by an alternative routine. Figure 3 shows the high-level structure of the controller, which is implemented in the rapid prototyping environment.

The input and the output module convert the signals to useful conditions for each side of the controller. The core of the ECS algorithm is within the intervention handler module.

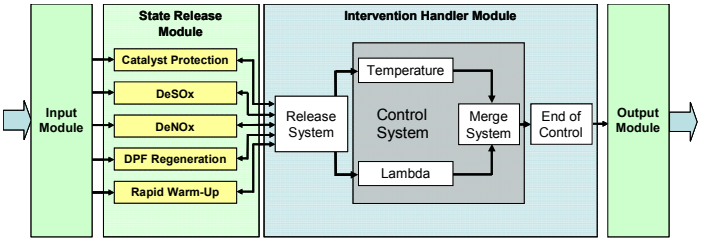

Figure 3: Emission control software structure

The different intervention requests coming from the state release module and a release system are transformed into the corresponding output signals through a multi-variable control structure. This allows simultaneous control of the temperature and lambda.

FUEL SPECIFICATIONS - Three different fuels were used in this study. The ultra-low-sulfur diesel fuel, or ULSD (also called the base fuel), was used to blend the 5% and 20% by volume blends (blended with soy methyl ester). Table 3 lists the fuel specifications for each tested fuel type. It is noteworthy that the B5 blend used a different base fuel, therefore some differences in the fuel properties are apparent.

Table 3: Fuel specifications

		ULSD	B5	B20
Net Heating Value	**MJ/kg**	42.534	42.432	41.522
Cetane Number	**-**	41.4	42.4	45.6
Density @ 293 K	**kg/m3**	847.5	847.9	852.9
K Viscosity @ 313 K	**mm2/sec**	2.429	2.335	2.685
Carbon	**wt%**	87.04	86.48	85.01
Oxygen	**wt%**	0.00	0.61	2.29
Hydrogen	**wt%**	12.96	12.91	12.70
H/C	**-**	1.774	1.779	1.780
O/C	**-**	0.00	0.01	0.02
Stochiometric Air/Fuel	**-**	14.46	14.36	14.04

TEST CYCLES

The project Included the following test cycles:

1. FTP-75, performed as two complete Urban Dynamometer Driving Schedule (UDDS) cycles
2. US06
3. HFET

Table 4 lists all the specifics of the test cycles, including length, average speed, and maximum speed.

Table 4: Test cycles

Cycle	Length	Average Speed	Maximum Speed	Remarks
UDDS	12.07 km 7.5 mi	31.6 km/h 19.6 mi/h	91.8 km/h 56.7 mi/h	Urban driving
US06	12.9 km 8.01 mi	77.9 km/h 48.4 mi/h	129.3 km/h 80.3 mi/h	Aggressive high-speed driving
HFET	16.52 km 10.26 mi	77.8 km/h 48.3 mi/h	96.4 km/h 59.9 mi/h	Highway driving, fuel economy

Figure 4 shows the cycles mentioned above.

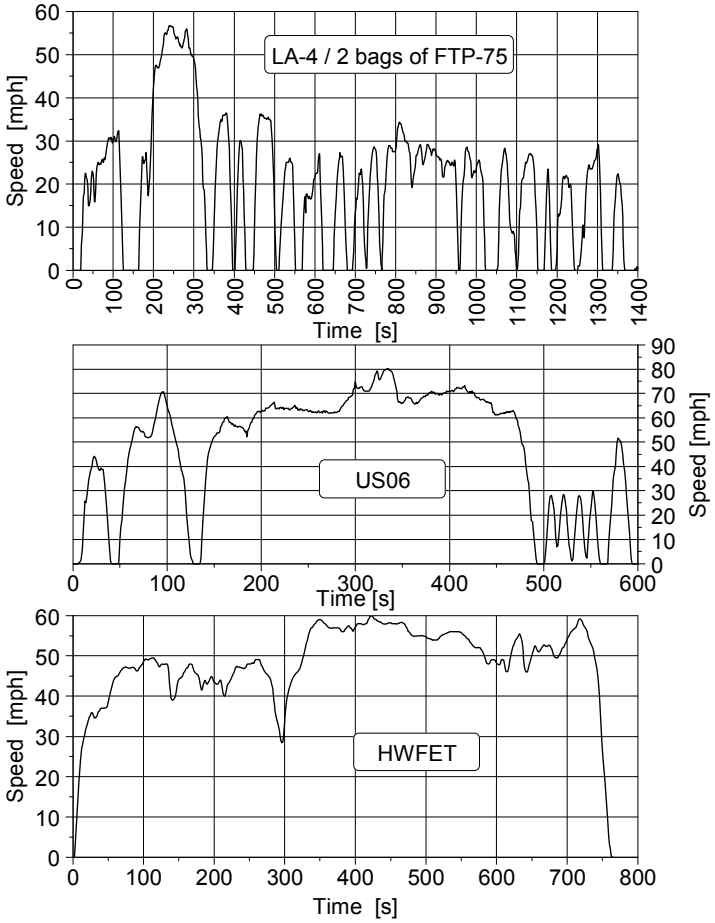

Figure 4: Emissions test cycles

In order to allow a direct comparison between the test cell and the vehicle, the torque and engine speed profile was programmed into the test cell control system. The base vehicle data were used to determine the power requirement as result of each cycle's vehicle speed profile. With the transmission gear and axle ratio, the transformation into engine speed and torque is performed. The refinement of the cycle results comparing the measured engine speed and commanded fuel quantity result was performed subsequently. The resulting test cycles performed in the test cell are described as *engine dynamometer transient cycle simulations,* and the vehicle tests are defined as *vehicle chassis dynamometer tests.*

DEVELOPMENT TEST RESULTS

COMPARISON OF ENGINE TEST CELL WITH VEHICLE RESULTS - To allow for accelerated development activities, the researchers found that duplication of the chassis dynamometer vehicle test cycles described in the previous section into the engine dynamometer environment benefits the calibration efforts. It was critical to develop cycles that not only matched the engine speed and load conditions in the same transient way as in the vehicle, but also to obtain the same engine-out emission levels as those of the vehicle. Figure 5 and Figure 6 show the engine speed and injected fuel quantity (equivalent to the load parameter) comparing the two different sites.

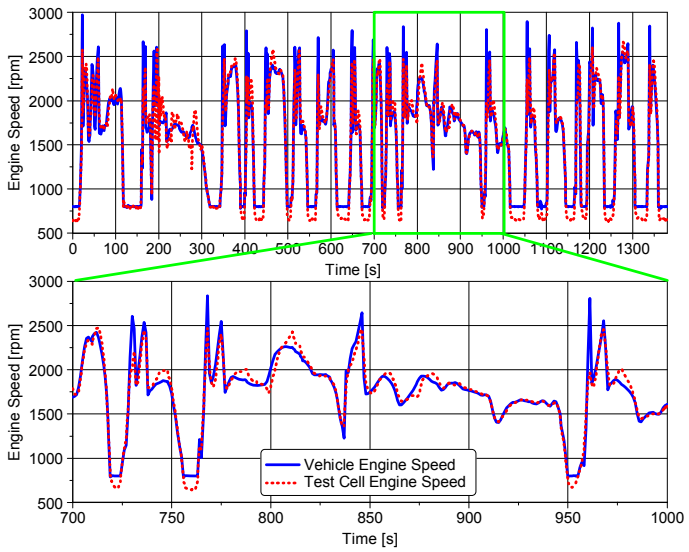

Figure 5: Engine speed comparison test cell and vehicle

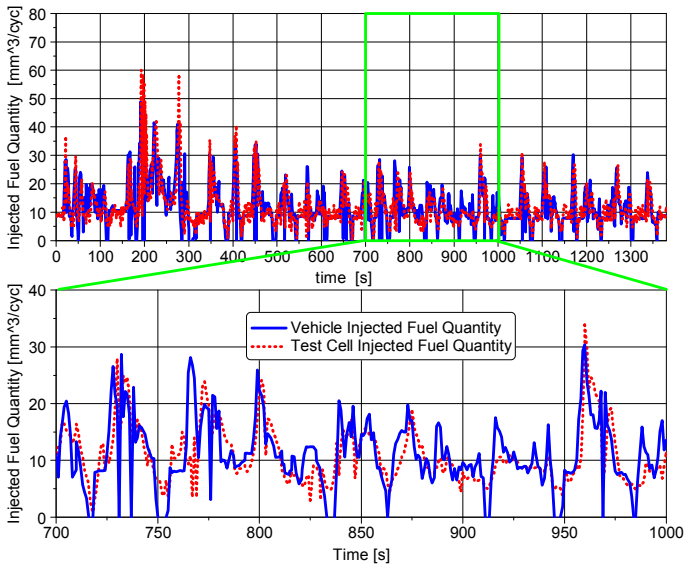

Figure 6: Fuel quantity comparison test cell and vehicle

The R^2 is greater than 0.95 for engine speed (comparing the engine dynamometer and the vehicle chassis dynamometer) and 0.60 for fuel quantity. The lower value for the fuel quantity is indicative of not full transient

operation in the engine dynamometer environment (quasi-transient, which excludes motoring phases during coasting). Despite the lower agreement of fuel-injection quantities, the main goal was to match the gaseous emissions, and NO_x in particular.

Figure 7 shows all gaseous emissions and compares the vehicle and engine dynamometer engine-out results. A 10% difference in engine-out NO_x emissions provides an acceptable accuracy for the development work. The largest difference between emissions was observed in the CO emissions. As this emission constituent is of secondary interest, no further efforts were undertaken to match this species any closer. All comparison tests were conducted with B20 fuel.

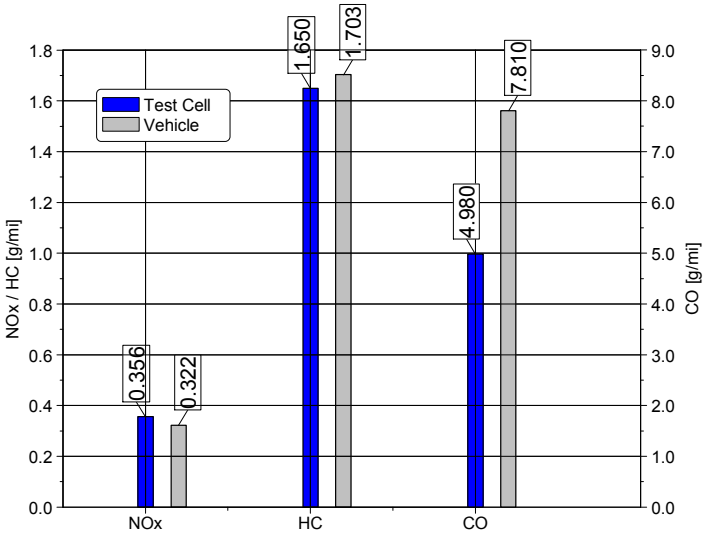

Figure 7: Base calibration tail-pipe emission comparison of engine test cell and vehicle (chassis test cell) for operation on B20

DPF REGENERATION DEVELOPMENT - The first phase of the development work was the calibration of the temperature control module for the DPF regeneration mode. This task has to precede all other activities, as the function of DPF regeneration allows for safe and continuous operation of all other system interventions. Development of the DPF regeneration strategy, as well as the calibration, were started under steady-state conditions in the test cell and were ultimately transferred to the vehicle.

As the project goal was the determination of the influences of biodiesel effects on engine and ECS, a mature emission control calibration—in this case, control of the DPF regeneration—was used to compare the ULSD base fuel with the B20 blend. Figure 8 and Figure 9 show the behavior of the two compared fuel blends at 600°C and 650°C (the tests were conducted in the engine dynamometer test cell). In both cases, the DPF was loaded to 5 g/L (5 grams of soot per liter of DPF volume). The soot burn-out rate was calculated based on the feedback signal from the differential pressure sensor. It is evident that, at the lower set-point temperature, the regeneration rate of the biodiesel blend is faster compared with that of the base fuel, as observed in previous studies [11]. This has been attributed to changes in particulate matter (PM) morphology and to the addition of oxygen to the PM surface, caused by the inclusion of biodiesel in the fuel. At the higher temperature set point, these differences disappear.

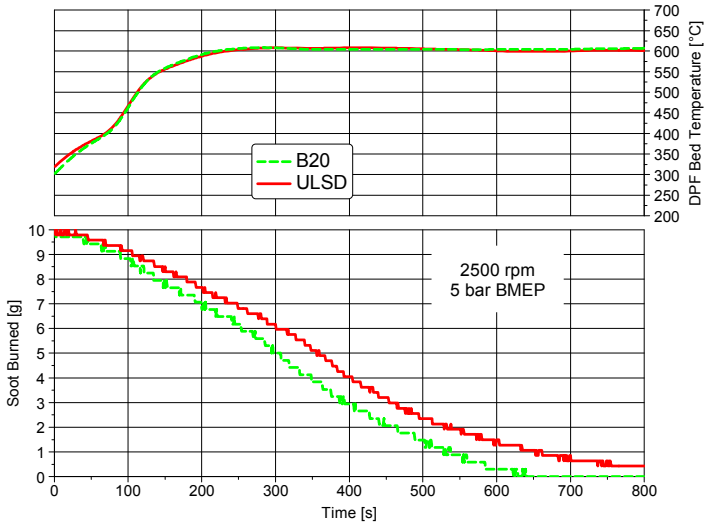

Figure 8: DPF regeneration at 600°C set point

The temperature increase upstream of the DPF was realized through a combination of air and fuel-handling parameter variations. The engine-out temperature is raised through intake air throttling in conjunction with lowered EGR rates. An early post injection (close to the main injection event) raises the engine-out temperature further, while a late-cycle post injection provides reactants to the DOC. This generates an exothermic reaction and controls the temperature at the set-point level.

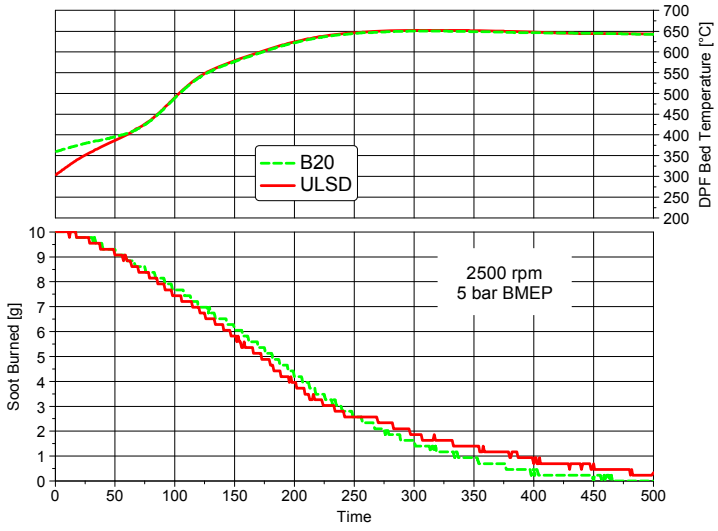

Figure 9: DPF regeneration at 650°C set point

The temperature control module was transferred to the vehicle and its performance evaluated under various driving conditions. The researchers found that, during transient operation, the control parameters had to be

recalibrated in order to obtain stable control of the DOC outlet temperature. Figure 10 and Figure 11 show the before- and after-calibration refinement results for typical city driving conditions in the vehicle. It was also necessary to slow down the temperature controller to avoid overshooting temperatures. With a slower control, the set point can be matched closely without significant over- or undershooting of the temperature.

The increase in the heat-up time is comparably small. The main parameters for these tests was a DPF loaded to 5 g/L. The vehicle speed ranged between 10 and 35 mph. The regeneration conditions were kept stable until complete regeneration was determined as a function of differential pressure.

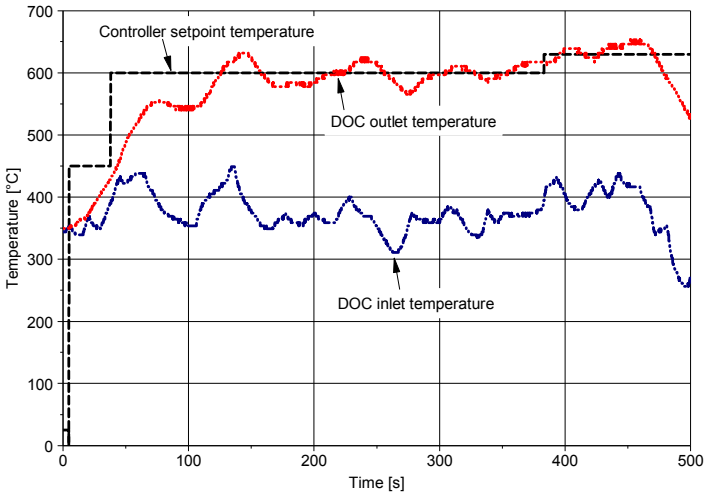

Figure 10: In-vehicle DPF regeneration before recalibration

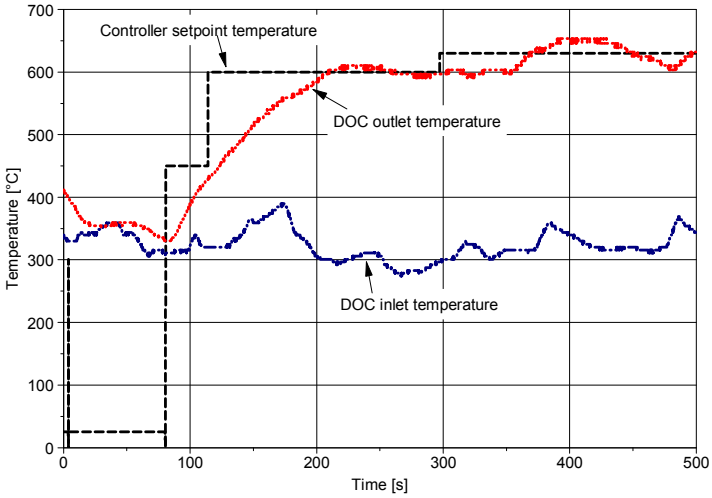

Figure 11: In-vehicle DPF regeneration after recalibration

NAC CALIBRATION AND DEVELOPMENT - NAC regeneration development is the cornerstone of meeting NO_x emission standards with the NAC system. A short pulse of rich exhaust gas desorbs the NO_x and subsequently reduces them, following the well-known chemistry of the three-way catalyst. The challenge is to obtain rich exhaust conditions with a diesel engine that typically operates under lean conditions.

The approach taken in this project was to utilize the multivariable controller, which allows the activation of all four actuator components (boost-pressure, EGR level, intake air throttling, and in-cylinder post injection) at the same time to adjust lambda to a given set-point value. The controller adjusts the setting for each parameter using a wide-range oxygen sensor as the feedback signal. The sensor is located upstream of the NAC.

A second wide-range oxygen sensor located downstream of the NAC serves as the controller feedback signal, determining the completion of the regeneration event. The downstream NAC lambda signal (lower portion of the graph) shows stoichiometric conditions until the regeneration is complete (time stamp 40.3 s) and then drops below $\lambda = 1$ (with an upstream NAC at $\lambda < 1$). This effect is used not only to control the NO_x regeneration, but also to effectively minimize the hydrocarbon breakthrough during these events.

Figure 12 shows the described effect, with the sensor signal upstream of the catalyst on the top portion of the graph and the downstream signal on the bottom.

The effect of the biodiesel in this example is negligible, as both lambda traces for ULSD as well as for the biodiesel blend are nearly identical. The investigation to determine fuel effects during the lean-rich transition was performed under numerous steady-state conditions covering a large area of the engine map, with the same results as those shown below.

In all cases, the lean duration was long enough to ensure fully saturated NAC. This was considered to be the only condition that allows repeatable results, as intermediate loading levels are difficult to maintain. The definition of fully saturated NAC was tail-pipe NO_x emission levels at or in excess of 80% of the engine-out NO_x level.

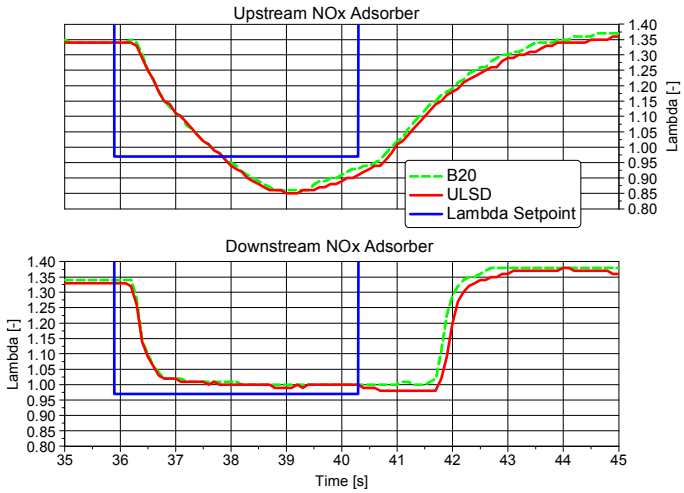

Figure 12: Biodiesel effects on lambda during lean-rich modulation (engine test cell)

Figure 13 shows the details of the actuator outputs during a lean-rich transition. In this case the effects of biodiesel are also evaluated. It is noteworthy that all the actuator commands that result in the rich pulse behave virtually identically for the two different fuels. As stated above, this investigation was performed in various operating conditions with similar results; that is, the different fuels had no impact on the emission controls in regard to the lean-rich modulation calibration.

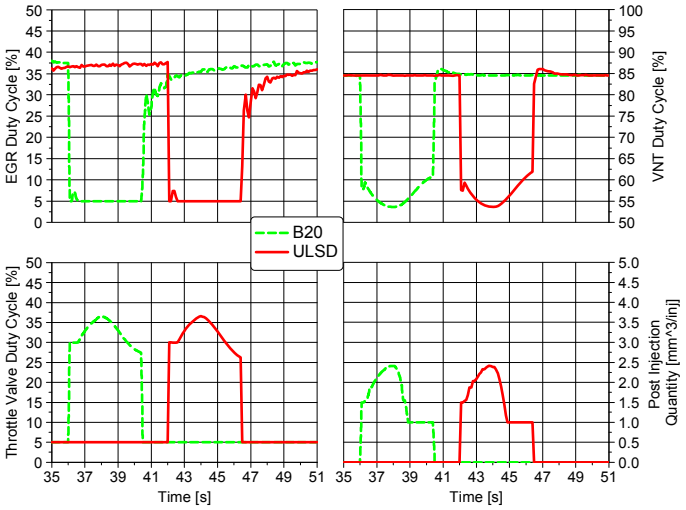

Figure 13: Biodiesel effects during lean-rich modulation (engine test cell)

For clarity, the traces for ULSD and biodiesel are offset by six seconds.

NAC DESULFURIZATION DEVELOPMENT - The basic principle of NAC catalysts is the adsorption of NO_2 during the lean operating phases of the engine. The NO_2 is adsorbed by alkali oxides forming nitrates such as $Ba(NO_3)_2$. The nitrates become unstable and release the NO and NO_2 under high temperature (thermal release of NO_x) or during rich exhaust conditions.

The rich exhaust conditions enable the utilization of the three-way catalyst mechanism to reduce the released NO_x into N_2 and CO_2. In addition to the desired functions, NAC exhibit the undesired function of adsorbing SO_3, forming $BaSO_4$, which is a considerably more stable compound requiring high temperatures and under-stoichiometric conditions to be released.

This release, often called desulfurization, has to occur frequently to avoid catalyst deactivation. The frequency of this event is dependent on the fuel sulfur level as well as the contribution of engine lubricating oil into the exhaust system.

The ECS layout, with the NAC upstream of the DPF, dictates a desulfurization strategy that switches continuously between lean and rich conditions under high temperatures. The switching is necessary to oxidize the undesired H_2S species. In the first step, the strategy and calibration were adjusted to steady-state operation.

Figure 14 shows the lambda, temperature, and emissions profile during one typical desulfurization process. The set-point temperature was at 680°C for the duration of the event. The lambda was transitioning between 1.4 and 0.8 to allow the most efficient sulfur removal under the rich conditions. There are trace-level H_2S emissions, and the sulfur is released as SO_2.

Apart from the heat-up phase, the hydrocarbon emissions are close to the detection level; however, even during this phase, hydrocarbon emissions stayed below 50 ppm. This strategy allowed sulfur removal rates approaching 90%, assuming retention levels of 100% during nondesulfurization operation at sulfur-loading levels of 1.5 g/L.

To accelerate the sulfur poisoning of the NAC, the engine was operated with high-sulfur diesel fuel until the target sulfur poisoning level was reached (in the present case, 1.5 g/L). Once the sulfur poisoning was complete, the fuel was switched back to B20 and the desulfurization experiment commenced.

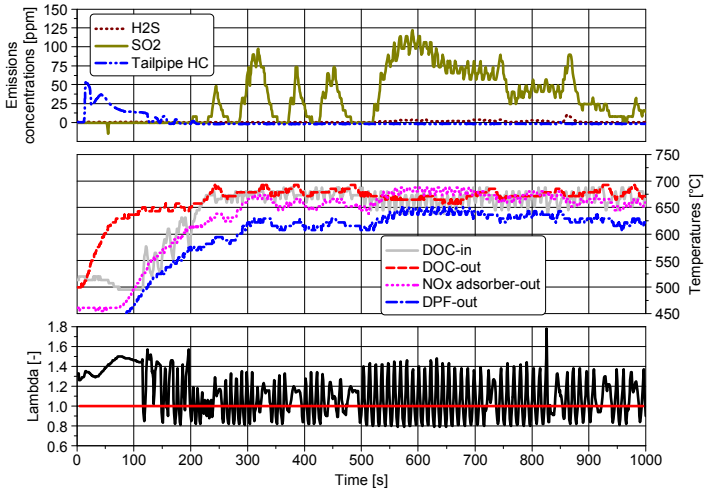

Figure 14: Desulfurization under steady-state conditions with B20 (engine test cell)

Figure 15 shows the desulfurization event during on-road vehicle operation. The vehicle was operated under city and freeway driving conditions, which required several complete vehicle stops. The peak vehicle speed during the present cycle was approximately 55 mph, with an average speed of about 30 mph.

The dynamics of the selected driving pattern forced the discontinuation of temperature and lambda control, in several cases. The control strategy attempts to maintain the highest possible temperature during these events to prevent the need for a repeated heat-up sequence.

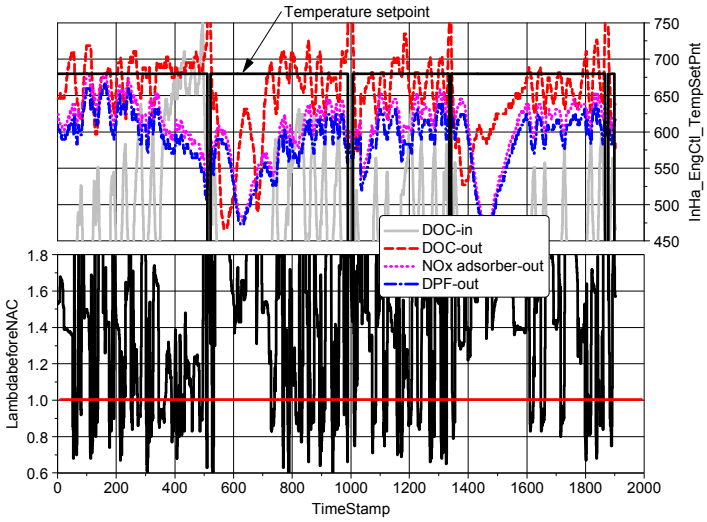

Figure 15: Desulfurization in-vehicle operation

No biodiesel effects were observed during the desulfurization development. As discussed in the previous section, the lean-rich modulation was also not affected by the differences in fuel properties. Since the desulfurization was conducted as lean-rich modulation under elevated temperatures, the conclusions from the NAC calibration development remain valid for the entire ECS function.

Effects that can result from the lower sulfur content were not observed, as the base fuel and the biodiesel blends contained very low sulfur levels. This makes determining differences as to the sulfur poisoning exceptionally challenging.

VEHICLE TEST RESULTS FOR NAC SYSTEM - All of the following vehicle tests were conducted at EPA's NVFEL in Ann Arbor, Michigan. The vehicle was tested using a 48-inch-diameter, single-roll, electric chassis dynamometer. Table 5 summarizes the analytical systems used for the vehicle tests.

Table 5: Summary of laboratory analytical equipment

Category	Analytical Equipment
CO	Horiba AIA-210/220 NDIR
CO_2	Horiba AIA-220 NDIR
HC	Horiba FIA-220 FID
CH_4	Horiba GFA-220 GC/FID
NO_x	Horiba CLA-220 CLD
THC	Horiba FIA-220 HFID
NO_x	Horiba CLA-220 HCLD
PM	EPA sampling system
CVS	Horiba VETS 9000 subsonic venturi

Three different fuels were evaluated during vehicle testing: ULSD, B5, and B20. Figure 16, Figure 17, and Figure 18 show the final results for the FTP75 testing portion. Investigators observed during these tests that NO_x tail-pipe emission numbers when the vehicle is running on B20 fuel are significantly more stable than when the vehicle is running on ULSD. The number of successful regenerations was higher for B20 fuel (B20: 10 regenerations for cold LA4, 8 for hot LA4; ULSD: 6 for cold/hot LA4). This is a result of the engine-out emission calibration, which was performed on a B20 fuel blend and thus is specifically optimized for this fuel.

Despite the fact that some characteristics of the B5 fuel blend did not fall within the trend between the ULSD and B20, some tendency toward increased tail-pipe NO_x emissions can be observed, from the B20 blend over the B5 fuel to the ULSD.

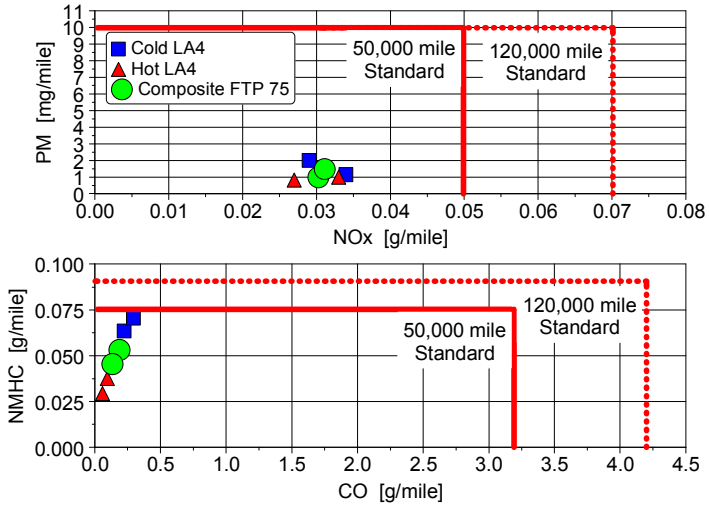

Figure 16: B20 emission results (UDDS)

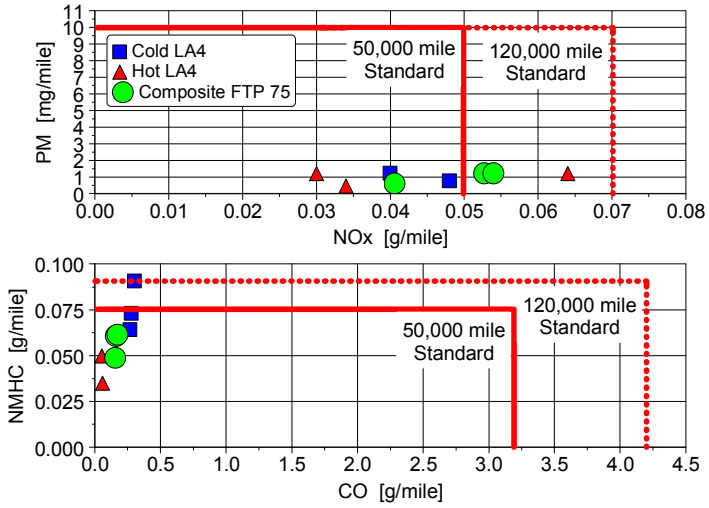

Figure 17: ULSD emission results with NAC system

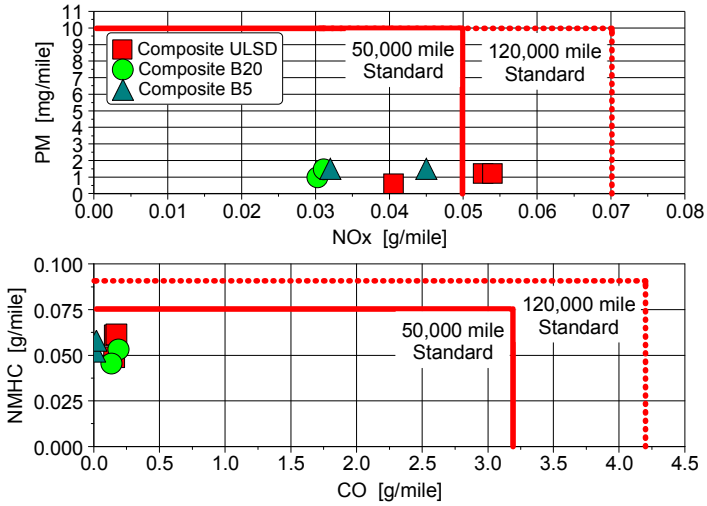

Figure 18: Composite emissions comparison with NAC system

The root cause of the higher NO_x emissions is illustrated in greater detail in Figure 19. The engine-out NO_x emissions are higher for the B20 fuel blend in comparison to the ULSD; this is similar to observations made in other testing [10]. It is important to note that this trend reverses at the tail-pipe-out location. This is the result of the higher exhaust temperature upstream of the NAC for ULSD. The temperature excursions above 450°C result in less favorable NO_x adsorption efficiencies with partial thermal desorption, during which the NO_x emissions increase. This is seen at time stamp 380 seconds in Figure 21.

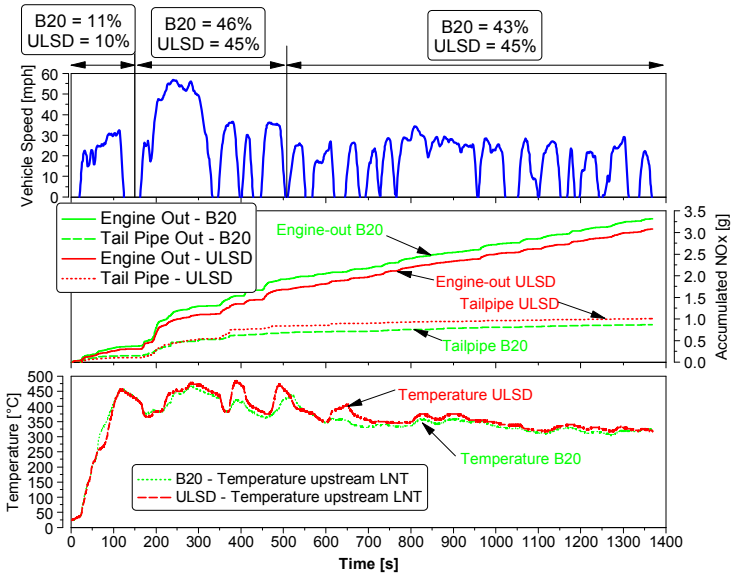

Figure 19: Temperature influence on NO_x emissions

Figure 20 shows the impact of the NO_x reduction on fuel economy and compares the B20 and the ULSD fuel. All data were measured at NVFEL. The base Euro 4 represents the engine calibration with the vehicle as delivered. It results in above 0.7 g/mile composite NO_x over the FTP75. The fuel economy is around 35 mpg, with some minor advantages for the B20 fuel. The initial calibration work focused on the reduction of engine-out NO_x in order to limit the emission control effectiveness requirements to below 90%.

The recalibration effort resulted in a reduction of more than 50% in NO_x and a fuel economy penalty of about 12%. The Tier 2 Bin 5 feed-gas emissions data were taken without any emission control interventions; therefore, the changes represent only the engine-out emission reduction effects.

The last comparison is with activated NAC regeneration controls, in which the NO_x levels drop below the 0.05 g/mile level to an overall reduction of more than 90%, compared with the base Euro 4 calibration. This additional NO_x control feature results in another fuel economy penalty of 2% to 3% in comparison to the feed-gas measurement without activated emission control.

The total NO_x reduction, which is in the mid-90% range, results in a total decrease in fuel economy of less than 14%. It is noteworthy that the NO_x emissions are higher for the B20 measurement as long as no emission controls were activated. This effect has been reported numerous times in different studies. The effect on fuel economy, however, is contrary to many reports on biodiesel operation. The following section discusses an in-depth investigation performed to isolate these effects.

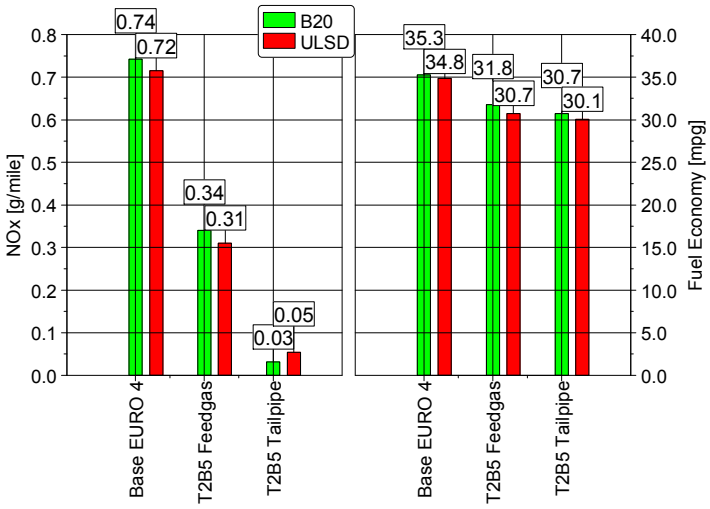

Figure 20: NO_x emission reduction and its impact on fuel economy

COMBUSTION ANALYSIS - The fuel economy numbers discussed in the previous section led to more detailed investigations to determine the root cause of improved fuel economy when a vehicle is operating with biodiesel fuel blends. This effect is counterintuitive, as B20 has a 2.5% lower heating value when compared with that of ULSD. The lower heating value typically results in a decrease in power output and thus an increase in specific fuel consumption.

Figure 21 shows the combustion comparison of the two different fuels at the same operating point on the engine map (1500 rpm, 15 mm^3/cycle fuel injection quantity

command → BMEP/IMEP [brake mean effective pressure/indicated mean effective pressure] varied as a function of combustion efficiency; see Table 6). The heat release rate and the total heat release were consistently higher for the biodiesel fuel. As a by-product of the faster combustion, the pressure rise rate was also higher. The analysis was applied to a wide range of the engine map and resulted in the same conclusion.

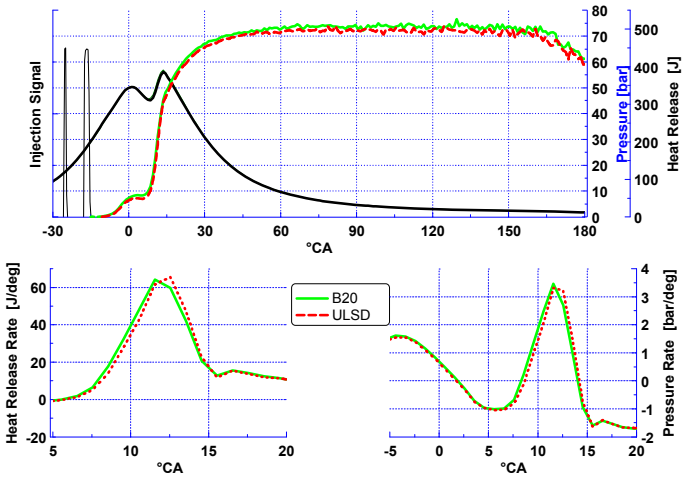

Figure 21: Combustion analysis 1500 rpm, 15 mm^3/cycle

Table 6 lists additional details that corroborate the findings discussed above. At the same commanded fuel quantity, the IMEP is approximately 2.5% higher, which is an indicator of higher combustion efficiency. The energy supplied is approximately 1.5% lower; however, this does not follow the 2.5% heating value reduction of the fuel specifications. The offset is a result of the increase in actual fuel quantity (due to the higher fuel density of the biodiesel fuel blend) injected into the cylinder, which compensates for 1% of the total energy difference.

The gaseous emissions are another indicator of higher combustion efficiency. Nitrogen oxides are significantly higher for operation on B20; HC and CO are elevated for operation on ULSD. The smoke number (as a combustion efficiency indicator) corroborates the superior combustion efficiency of biodiesel fuel blends.

Table 6: Combustion analysis of B20 vs. ULSD

	B20	ULSD
IMEP [bar]	5.75	5.61
Injection mass [mg/cyc]	13.119	13.051
Mass burn Efficiency [%]	92.04	88.63
Energy supplied [J/cyc]	546.35	555.13
NOx [ppm]	102.59	76.96
CO [ppm]	648.23	852.91
HC [ppm]	165.02	269.16
Smoke [FSN]	0.55	1.08

AGING TEST RESULTS

AGING PROTOCOL - The goal of the aging part of the project was to develop ECS parts that are aged to an equivalent of 120,000 miles, or full useful life. To accomplish this, the engine and ECS were exposed to an equivalent useful lifetime of fuel in the engine dynamometer test cell.

To keep the aging time at a reasonable level, the aging duration for each ECS was set to approximately 700 hours. The following assumptions were used regarding fuel consumption for the system:

- Highway cycle fuel economy at 55 mpg
- City cycle fuel economy at 33 mpg
- Split of ¾ highway and ¼ city cycle

These assumptions resulted in an average fuel economy of 49.5 mpg. At 120,000 miles, this equates to 2,424 gallons (7,708 kg) of fuel. With 700 hours of aging time, an average fuel consumption of approximately 11 kg/h was established. Three operating phases were established to reflect real in-use operating modes:

1. NAC operation using the systems efficiency control algorithms to determine the frequency of regeneration events
2. DPF regeneration (300 for full useful life)
3. Desulfurization (25 for full useful life).

Table 7 shows the detailed operating conditions and durations for the durability cycle chosen. In phase 1, the engine operating conditions are changed between two operating points (OP1 and OP2) for 120 minutes. In the second phase, the system transitions into the DPF regeneration mode with a DPF inlet temperature set point of 650°C.

Once the DPF regeneration is completed, the system returns to phase 1 operation. This sequence is repeated until a total run time of 28 hours is reached. After 28 hours, the system is forced into the desulfurization mode with a set-point temperature of 700°C and frequent lean-rich transitions, as described in the section on NAC desulfurization development.

In addition to the operating point discussion, Table 7 also contains temperature information for different emission control components. It also includes fuel flow rates for each state.

Table 7: Detailed operating conditions for durability cycle

	Duration [min]	Total number of times to be repeated	Temperature NAC [°C]	Temperature DPF [°C]	Total Fuel Consumption [gal]
OP 1 (2000 rpm, 210 Nm)	5		492.90	457.87	0.262
OP 2 (2600 rpm, 160 Nm)	5		469.99	456.90	0.287
Phase 1 [OP1x12+OP2x12]	120	300	481.45	457.38	6.234
Phase 2 [DPF regeneration] (2600 rpm, 110 Nm)	20	300	630.00	610.00	1.062
Total per cycle (Phase 1 + Phase 2)	140	300	555.72	533.69	7.296
Phase 3 (Desulphurization) (2200 rpm, 75 Nm)	20	25	675.00	600.00	0.668
Total hours of running	**708 hrs**		**Total fuel for durability test**		**2206 gal**

Figure 22 shows an overview of the various parameters measured during the durability cycle. Overall, 708 hours of durability test time were conducted; 311 DPF regeneration events and 28 desulfurization events were initiated and successfully completed.

The average catalyst temperatures are shown at the bottom of the graph for the different events. The desulfurization showed the highest catalyst bed temperatures, at around 650°C in the NAC. The DPF regeneration temperature averaged below 630°C for the NAC and a little above 610°C for the DPF (the set-point temperature was set to 600°C). During operation in phase 1 and 2 or conventional NAC regeneration operation, the temperatures averaged between 460°C and 500°C.

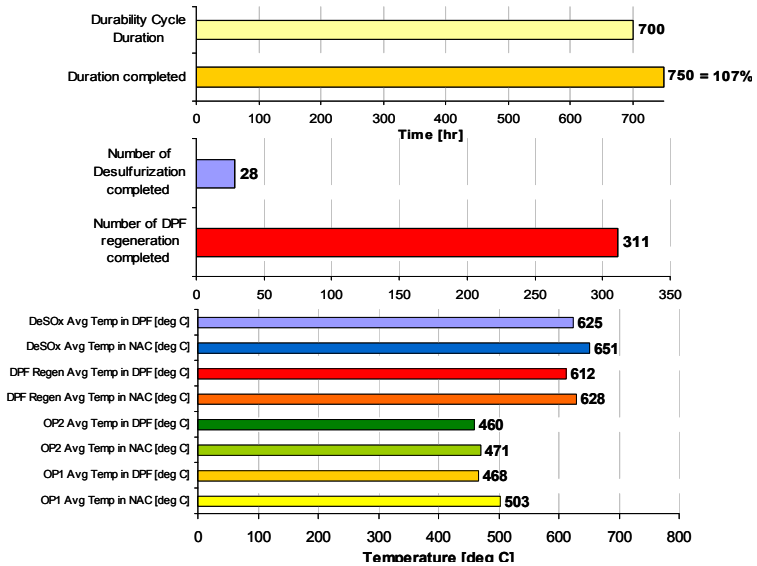

Figure 22: Durability test statistics

EMISSION RESULTS FOR DURABILITY COMPONENTS - During the aging of the engine and emission control system, three evaluation sequences were initiated to allow the assessment of system deterioration. The 0-hour (0-h) and 350-h (intermediate useful life) evaluation tests were performed in an engine dynamometer test cell simulating the various certification cycles. The end-of-life or useful life test was conducted at NVFEL.

Figure 23 shows the 0-h and intermediate useful life results as conversion efficiencies. Since these tests were performed in an engine dynamometer test cell with elevated engine-out NO_x emissions, the tail-pipe results do not represent the total system performance potential.

The graph shows conversion efficiency requirements, with system and engine-out emissions as developed. For both the 0-h and the 350-h evaluation period, the conversion efficiencies met the requirements. This indicates that the system installed in the vehicle could meet emission standards for 50,000 miles.

The final emission tests were performed in the vehicle and are presented in Figure 24. The 0-h results are well within the emission standard for 50,000 miles, while the intermediate useful life fails the 0.05 g/mile test as a result of increased engine-out NO_x emissions for the durability engine. The final emission evaluation in the vehicle shows that all emissions are within the 120,000-mile standard. The nonmethane hydrocarbon, or NMHC, emissions are below 50,000 miles, which is an indicator of successful hydrocarbon control during the lean-rich modulation.

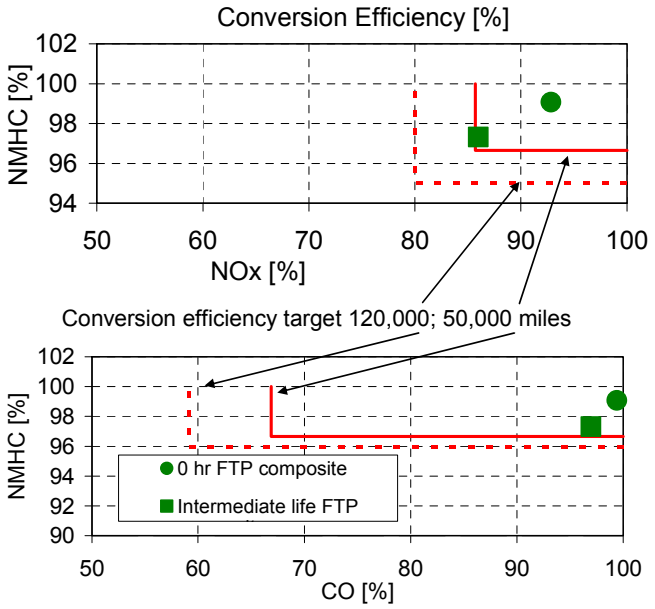

Figure 23: Zero hours and intermediate useful life emission results over the FTP

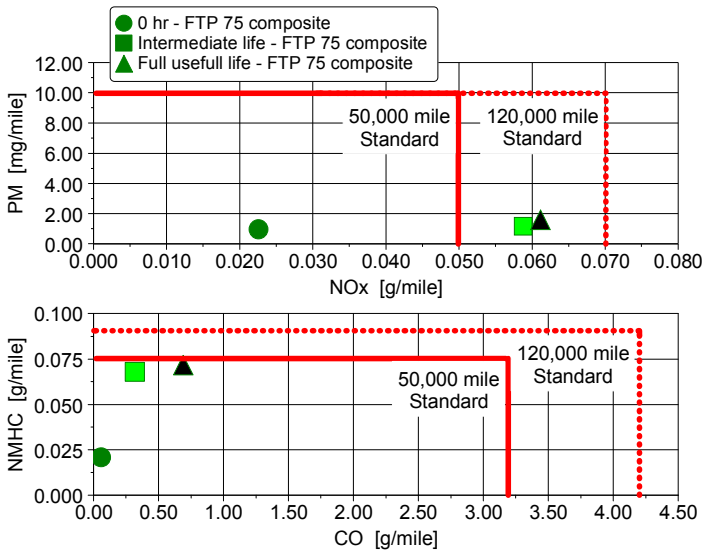

Figure 24: System performance evaluation

CONCLUSIONS

The following are the main conclusions derived from this work to date:

- Under normal operating conditions, biodiesel has marginal impact on DPF regeneration rates. The effects are more pronounced at low lambda rates and lower temperatures, at which biodiesel shows some benefits in regeneration rate in comparison to that of ULSD.
- No impact was observed for biodiesel fuel blends during the NAC lean-rich cycle development. The multivariable control resulted in virtually identical actuator settings with the same set point. The investigations were performed throughout the engine map with the same result.
- No effects could be observed for biodiesel during the desulfurization mode.
- Vehicle results showed some benefits for a vehicle operating on B20 fuel blend with the NAC system. This is a result of the calibration work being performed using the 20% biodiesel fuel blend. The resulting higher exhaust temperatures with ULSD resulted in lower NAC system effectiveness.
- The NO_x adsorber ECS aged to intermediate useful life showed efficiencies in the mid-80% range, thus allowing operation within the emission standards.
- The NO_x adsorber system aging was performed using the B20 fuel blend. The system deteriorated while still allowing it to meet Tier 2 Bin 5 levels at useful life conditions.

ACKNOWLEDGMENTS

The authors hereby would like to express their gratitude to all participating team members that supported the project and actively contributed in all technical discussions.

This work was jointly supported by the United Stated Department of Energy, Office of Vehicle Technologies Programs and by the National Biodiesel Board. Special thanks to Stephen Goguen, Kevin Stork, and Dennis Smith of the U.S. DOE, and Steve Howell at NBB.

Also, thanks to Joe Kubsh and Rasto Brezny of MECA and its team members for the in-kind contributions of all exhaust aftertreatment hardware and to Charles Schenk of the U.S. EPA for providing the opportunity for the vehicle tests.

REFERENCES

1. Tomazic, D., Tatur, M., Thornton, M. “Development of a Diesel Passenger Car Meeting Tier 2 Emissions Levels,” SAE Paper 2004-01-0581, March 2004, Detroit, Michigan.
2. Tomazic, D., Tatur, M., Thornton, M. “APBF-DEC NO_x Adsorber/DPF Project: Light-Duty Passenger Car Platform,” DEER Paper, August 2003, Newport, Rhode Island.
3. Geckler, S., Tomazic, D., et al. “Development of a Desulfurization Strategy for a NO_x Adsorber Catalyst System,” SAE Paper 2001-01-0510, March 2001, Detroit, Michigan.
4. McDonald, J. “Progress in the Development of Tier 2 Light-Duty Diesel Vehicles,” SAE Paper 2004-01-1791, March 2004, Detroit, Michigan.
5. Webb, C., et al. “Achieving Tier 2 Bin 5 Emission Levels With a Medium-Duty Diesel Pick-Up and a NO_x Adsorber, Diesel Particulate Filter Emissions System-Exhaust Gas Temperature Management,” SAE Paper 2004-01-0584.
6. Whitacre, S., et al. “Systems Approach to Meeting EPA 2010 Heavy-Duty Emission Standards Using a NO_x Adsorber Catalyst and Diesel Particle Filter on a 15l Engine,” SAE Paper 2004-01-0587.
7. Tatur, M., Tyrer, H., Tomazic, D., Thornton, M., McDonald, J. “Tier 2 Intermediate Useful Life (50,000 miles) and 4000 Mile Supplemental Federal Test Procedure (SFTP) Exhaust Emission Results for a NO_x Adsorber and Diesel Particle Filter Equipped Light-Duty Diesel Vehicle,” SAE Paper 2005-01-1755.
8. Thornton, M., Tatur, M., Tyrer, H., Tomazic, D. “Full Useful Life (120,000 miles) Exhaust Emission Performance of a NO_x Adsorber and Diesel Particle Filter Equipped Passenger Car and Medium-Duty Engine in Conjunction with Ultra Low Sulfur Fuel,” DEER 2005.
9. Tyson, K.S., Bozell, J., Wallace, R., Petersen, E., Moens, L. “Biomass Oil Analysis: Research Needs and Recommendations”, NREL Technical Report

TP-510-34796, National Renewable Energy Laboratory, June 2004.
10. McCormick, R.L., Williams, A., Ireland, J., Brimhall, M., and Hayes, R.R. *Effects of Biodiesel Blends on Vehicle Emissions*, NREL Milestone Report MP-540-40554, National Renewable Energy Laboratory, October 2006.
11. Sheehan, J., Camobreco, V., Duffield, J., Graboski, M., Shapouri, H. *An Overview of Biodiesel and Petroleum Diesel Life Cycles*, NREL Report TP-580-24772, National Renewable Energy Laboratory, May 1998.
12. Williams, A., et al. "Effect of Biodiesel Blends on Diesel Particulate Filter Performance," SAE 2006-01-3280.

CONTACT

Marek Tatur, FEV Inc., Department Manager, Diesel Engines. E-Mail: tatur@fev-et.com

DEFINITIONS, ACRONYMS, ABBREVIATIONS

BTDC: before top dead center
B20: biodiesel with 20% renewable fuels content
B5: biodiesel with 5% renewable fuels content
CA: crank angle
CO: carbon monoxide
CO_2: carbon dioxide
CDPF: catalyzed diesel particle filter
DOE: U.S. Department of Energy
DPF: diesel particle filter
ECM: electronic control module
ECS: emission control system
ECU: engine control unit
EGR: exhaust gas recirculation
EPA: U.S. Environmental Protection Agency
FSN: filter smoke number
FTP: Federal Test Procedure
h hour
HC: hydrocarbon
HD: heavy-duty
HFET: Highway Fuel Economy Test
HSDI: high-speed direct injection
LA4: Urban Dynamometer Driving Schedule (UDDS)
NAC: NO_x adsorber catalyst
NMHC: nonmethane hydrocarbon
NO: nitric oxide
NO_2: nitrogen dioxide
NO_x: oxides of nitrogen
O_2 oxygen
OEM: original equipment manufacturer
PM: particulate matter
PCR: (boost) pressure control regulator
RPM: revolutions per minute (engine speed)
SCR: selective catalytic reduction
SET: Supplemental Emissions Test
SFI: secondary fuel injector
THC: total hydrocarbon
TV: throttle valve
UDDS: Urban Dynamometer Driving Schedule
ULSD: ultra-low-sulfur diesel (here, the base fuel)
VNT: variable nozzle turbine

REPORT DOCUMENTATION PAGE

Form Approved
OMB No. 0704-0188

PLEASE DO NOT RETURN YOUR FORM TO THE ABOVE ORGANIZATION.

1. REPORT DATE *(DD-MM-YYYY)*	2. REPORT TYPE	3. DATES COVERED *(From - To)*
August 2008	Conference Paper	

4. TITLE AND SUBTITLE
Effects of Biodiesel Operation on Light-Duty Tier 2 Engine and Emission Control Systems: Preprint

5a. CONTRACT NUMBER
DE-AC36-99-GO10337

5b. GRANT NUMBER

5c. PROGRAM ELEMENT NUMBER

6. AUTHOR(S)
M. Tatur, H. Nanjundaswamy, D. Tomazic, and M. Thornton

5d. PROJECT NUMBER
NREL/CP-540-42928

5e. TASK NUMBER
FC089400

5f. WORK UNIT NUMBER

7. PERFORMING ORGANIZATION NAME(S) AND ADDRESS(ES)
National Renewable Energy Laboratory
1617 Cole Blvd.
Golden, CO 80401-3393

8. PERFORMING ORGANIZATION REPORT NUMBER
NREL/CP-540-42928

9. SPONSORING/MONITORING AGENCY NAME(S) AND ADDRESS(ES)

10. SPONSOR/MONITOR'S ACRONYM(S)
NREL

11. SPONSORING/MONITORING AGENCY REPORT NUMBER

12. DISTRIBUTION AVAILABILITY STATEMENT
National Technical Information Service
U.S. Department of Commerce
5285 Port Royal Road
Springfield, VA 22161

13. SUPPLEMENTARY NOTES

14. ABSTRACT *(Maximum 200 Words)*

Interest in diesel-powered cars is rising in the United States, along with the desire to reduce the nation's dependence on imported petroleum. As a result, operating diesel vehicles on fuels blended with biodiesel is also gaining attentiion. One of several factors to consider when operating a vehicle on biodiesel blends is understanding the performance and impact of the fuel on the emission control system. This paper documents the impact of biodiesel blends on engine-out emissions as well as overall system performance in terms of emissions control system calibration and overall system efficiency.

15. SUBJECT TERMS
biodiesel; diesel-powered vehicles; engine-out emissions; light-duty vehicles; emissions control system; biodiesel blends;

16. SECURITY CLASSIFICATION OF:			17. LIMITATION OF ABSTRACT	18. NUMBER OF PAGES	19a. NAME OF RESPONSIBLE PERSON
a. REPORT	b. ABSTRACT	c. THIS PAGE			
Unclassified	Unclassified	Unclassified	UL		19b. TELEPHONE NUMBER (*Include area code*)

Standard Form 298 (Rev. 8/98)
Prescribed by ANSI Std. Z39.18